

Letter of Intent: A new investigation of  $\nu_\mu \rightarrow \nu_e$  oscillations with improved sensitivity in an enhanced MiniBooNE experiment

**MiniBooNE Collaboration**

R. Dharmapalan, S. Habib, C. Jiang, & I. Stancu  
*University of Alabama, Tuscaloosa, AL 35487*

Z. Djurcic  
*Argonne National Laboratory, Argonne, IL 60439*

R. A. Johnson & A. Wickremasinghe  
*University of Cincinnati, Cincinnati, OH 45221*

G. Karagiorgi & M. H. Shaevitz  
*Columbia University, New York, NY 10027*

B. C. Brown, F.G. Garcia, R. Ford, W. Marsh, C. D. Moore,  
D. Perevalov, & C. C. Polly  
*Fermi National Accelerator Laboratory, Batavia, IL 60510*

J. Grange, J. Mousseau, B. Osmanov, & H. Ray  
*University of Florida, Gainesville, FL 32611*

R. Cooper, R. Tayloe  
*Indiana University, Bloomington, IN 47405*

G. T. Garvey, W. Huelsnitz, W. C. Louis, C. Mauger, G. B. Mills,  
Z. Pavlovic, R. Van de Water, & D. H. White  
*Los Alamos National Laboratory, Los Alamos, NM 87545*

R. Imlay, M. Tzanov  
*Louisiana State University, Baton Rouge, LA 70803*

L. Bugel, J. M. Conrad  
*Massachusetts Institute of Technology, Cambridge, MA 02139*

B. P. Roe  
*University of Michigan, Ann Arbor, MI 48109*

A. A. Aguilar-Arevalo  
*Instituto de Ciencias Nucleares, Universidad Nacional Autónoma de México,  
México D.F. México*

P. Nienaber  
*Saint Mary's University of Minnesota, Winona, MN 55987*

October 29, 2018

## Abstract

We propose adding 300 mg/l PPO to the existing MiniBooNE detector mineral oil to increase the scintillation response. This will allow the detection of associated neutrons and increase sensitivity to final-state nucleons in neutrino interactions. This increased capability will enable an independent test of whether the current excess seen in the MiniBooNE oscillation search is signal or background. In addition it will enable other neutrino interaction measurements to be made including a search for the strange-quark contribution to the nucleon spin ( $\Delta s$ ) and a low-energy measurement of charged-current quasielastic scattering.

## Contents

<b>1</b>	<b>Executive Summary</b>	<b>3</b>
<b>2</b>	<b>Introduction</b>	<b>4</b>
<b>3</b>	<b>Physics Goals</b>	<b>6</b>
3.1	Oscillation search with CC/NC identification . . . . .	6
3.2	Proton to neutron ratio in NC elastic events . . . . .	7
3.3	A measurement of $\nu_\mu$ $^{12}\text{C} \rightarrow \mu^-$ $^{12}\text{N}_{\text{g.s.}}$ . . . . .	7
3.4	A test of the QE assumption in neutrino energy reconstruction . . . . .	8
<b>4</b>	<b>Increasing scintillation in MiniBooNE</b>	<b>9</b>
4.1	Neutron capture . . . . .	9
4.2	Scintillation light in MiniBooNE, currently . . . . .	9
4.3	Simulations of increased scintillation light . . . . .	10
4.4	Event reconstruction . . . . .	11
4.5	Determination of the scintillator cocktail . . . . .	16
<b>5</b>	<b>Simulated oscillation analysis</b>	<b>18</b>
5.1	Measuring the neutron fraction in oscillation candidate events . . . . .	18
5.2	Variations of study assumptions . . . . .	20
5.3	Calibration of the neutron fraction in NC and CC events . . . . .	21
<b>6</b>	<b>Implementation</b>	<b>23</b>
6.1	Suggested plan for adding scintillator . . . . .	23
6.2	Detector changes . . . . .	23
6.3	Run plan . . . . .	23
6.4	Future Work . . . . .	23
<b>7</b>	<b>Conclusions and request</b>	<b>25</b>

# 1 Executive Summary

In this Letter, we describe a plan for adding scintillator to the existing MiniBooNE mineral oil detector medium to allow a test of the neutral-current/charged-current (NC/CC) nature of the MiniBooNE low-energy excess. The scintillator will enable reconstruction of 2.2 MeV  $\gamma$  from neutron-capture on protons following neutrino interactions. Charged-current neutrino interactions, at low-energy where the MiniBooNE oscillation excess is observed, should have associated neutrons with less than 10% probability. This is in contrast to the neutral-current backgrounds which should have associated neutrons in approximately 50% of events. These predicted neutron fractions will be measured in MiniBooNE for both the charged- and neutral-current channels, thereby eliminating that systematic uncertainty. A measurement of the neutron-fraction in a new appearance oscillation search with MiniBooNE will increase the significance of the oscillation excess, if it maintains in the new data set, to at minimum  $5\sigma$ .

This new phase of MiniBooNE will enable additional important studies such as the spin structure of nucleon ( $\Delta s$ ) via NC elastic scattering, a low-energy measurement of the neutrino flux via  $\nu_\mu \ ^{12}\text{C} \rightarrow \mu^- \ ^{12}\text{N}_{\text{g.s.}}$  scattering, and a test of the quasielastic assumption in neutrino energy reconstruction. These topics will yield important, highly-cited results over the next 5 years for a modest cost, and will help to train Ph.D. students and postdocs.

This enterprise will offer complementary information to that from the upcoming MicroBooNE experiment. MicroBooNE uses an Argon target, and it will be helpful to further study the MiniBooNE excess with new methods but using the same carbon nucleus. In addition, the beam will be delivering neutrinos for MicroBooNE, so there is minimal incremental cost to also deliver beam to MiniBooNE.

*This program of measurements requires approximately  $6.5 \times 10^{20}$  protons on target delivered to MiniBooNE and can begin in early 2014. We are requesting support of this concept to enable the collaboration to plan the experiment and analysis in more detail with the goal of submitting a full proposal for the experiment in mid-2013.*

## 2 Introduction

The MiniBooNE experiment has, for the last 10 years, searched for  $\nu_\mu \rightarrow \nu_e$  and  $\bar{\nu}_\mu \rightarrow \bar{\nu}_e$  in the Booster Neutrino Beamline at Fermilab. The beam was shut down in April 2012 to enable the Fermilab accelerator complex to be upgraded in preparation for delivering higher beam power to the NOvA experiment. Before the shutdown, MiniBooNE completed an antineutrino phase of running which brought the total amount of beam delivered to the experiment to  $11.3 \times 10^{20}$  protons on target (POT) in antineutrino mode and  $6.5 \times 10^{20}$  POT in neutrino mode.

Both  $\nu_\mu \rightarrow \nu_e$  and  $\bar{\nu}_\mu \rightarrow \bar{\nu}_e$  oscillation analyses have been conducted with this data individually [1]-[4] and recently as a combined data set with the latest updates to the antineutrino data [5]. There is an excess of events over the calculated background in both modes (Fig. 1) examined individually as well as for the combined data set which contains a total excess of  $240.3 \pm 62.9$  ( $3.8\sigma$ ) events. A two-neutrino fit to the combined data set yields allowed parameter regions (Fig. 2) which are consistent with oscillations in the 0.01 to 1  $\text{eV}^2$   $\Delta m^2$  range and are consistent with the regions reported by the LSND experiment [6].

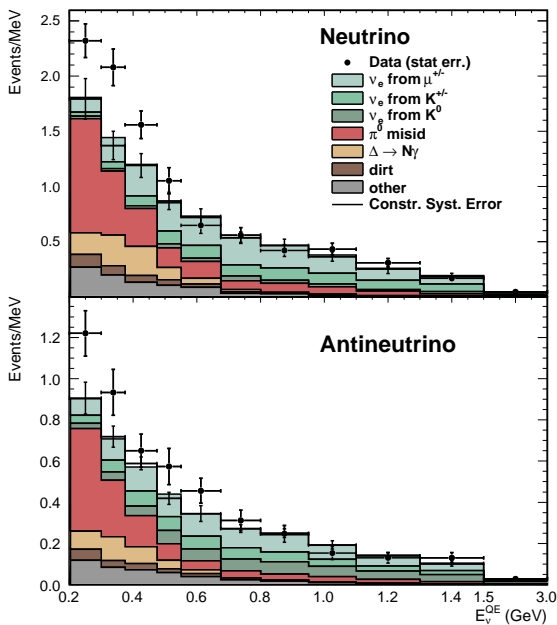


Figure 1: The neutrino mode (top) and antineutrino mode (bottom) reconstructed neutrino energy,  $E_\nu^{QE}$ , distributions for data (points with statistical errors) and predicted background (histogram with systematic errors).

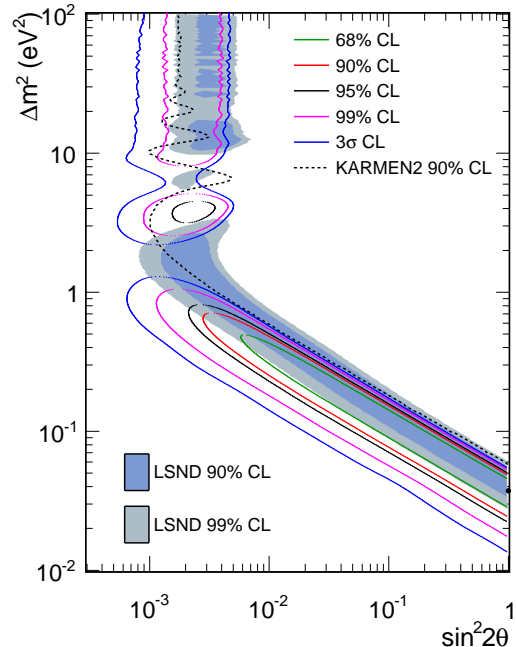


Figure 2: MiniBooNE allowed regions in combined neutrino and antineutrino mode for events with  $200 < E_\nu^{QE} < 3000$  MeV within a  $2\nu$  oscillation model.

The excess occurs in both  $\nu$  and  $\bar{\nu}$  samples at low energy, and so it is natural to consider more carefully the largest backgrounds in that energy region. They are dominated by neutral-current (NC)  $\pi^0$  and NC  $\Delta$  radiative decays ( $\Delta \rightarrow N\gamma$ ). Both of these NC processes are constrained by measurements within MiniBooNE, but an anomalous process such as NC  $\gamma$  production, not sufficiently accounted for in the MiniBooNE analysis, could lessen the significance of the oscillation excess. We are proposing to measure these backgrounds with a new technique combined with

additional running of MiniBooNE.

The MiniBooNE detector uses 800 tons of mineral oil ( $\text{CH}_2$ ) as a target medium for inducing CC and NC neutrino interactions. The mineral oil also serves as the detector medium for observing the final state particles resulting from the interactions. This is achieved via detection of the Cerenkov light from charged particles in the 1280 8" photomultiplier tubes (PMTs) that line the inside of the spherical detector tank. In addition to the Cerenkov light produced in a cone around the trajectory of charged particles, some isotropic scintillation light is produced due to presence of aromatic impurities in the mineral oil.

We propose adding approximately 300 kg of PPO scintillator to the 800 tons of MiniBooNE mineral oil to increase the amount of scintillation light produced by 2.2 MeV  $\gamma$  that result from delayed ( $\tau \approx 186 \mu\text{s}$ ) neutron capture on protons within the mineral oil. This will allow an important test of the oscillation signal by checking that the excess is indeed due to CC interactions of low-energy neutrinos and not an incorrectly calculated NC background. This can be done by counting  $n$ -capture events that follow oscillation candidate events. If the excess is indeed due to CC interactions of low energy  $\nu_e$ , only approximately 10% of the excess will have associated  $n$ -capture events. If, instead, the excess is due to a NC process, one would expect many more neutrons produced since the interactions are caused from higher energy neutrinos. One expects approximately 50% of NC background events to have an associated neutron. An attractive feature of this method is that the neutron fraction for CC and NC processes may be measured with MiniBooNE via similar channels thereby eliminating that systematic uncertainty.

The increased level of scintillation will enable several other important measurements. The detection of  $n$ -capture enables a measurement of the neutron to proton ratio in NC elastic scattering which is sensitive to the strange-quark spin of the nucleon ( $\Delta s$ ). The  $\beta$  decay from the  $^{12}\text{N}_{\text{g.s.}}$  in the  $\nu_\mu \text{ }^{12}\text{C} \rightarrow \mu^- \text{ }^{12}\text{N}_{\text{g.s.}}$  process will be better reconstructed which will allow a measurement of this process and a check of the low-energy neutrino flux. Low-energy recoil nucleons will be more visible within neutrino events allowing a test of the quasielastic assumption in neutrino energy reconstruction.

In the following sections, we describe the extended physics program that is made possible with the addition of scintillator to MiniBooNE. We will discuss how the scintillation light will be increased, how it affects event reconstruction, and describe a plan for future running with MiniBooNE in this new configuration.

### 3 Physics Goals

A main motivation for adding scintillator to MiniBooNE is to provide a test of the nature of the low-energy excess of events observed in both the  $\nu_e$  and  $\bar{\nu}_e$  appearance searches conducted by MiniBooNE. The addition of scintillator will also enable an investigation of the strange-quark contribution to the nucleon spin ( $\Delta s$ ), a measurement of the  $\nu_\mu$   $^{12}\text{C} \rightarrow \mu^-$   $^{12}\text{N}$  reaction, and a test of the quasielastic assumption in neutrino energy reconstruction.

#### 3.1 Oscillation search with CC/NC identification

MiniBooNE has measured a  $3.8\sigma$  excess of oscillation candidate events in the combined  $\nu_\mu$  and  $\bar{\nu}_\mu$  data sets collected to date at Fermilab [5]. As can be seen in Fig. 1, the predicted backgrounds in the low energy regions, where the excess is most substantial, are dominated by neutral current backgrounds. These are from two major sources, both from NC interactions: misidentification of the  $\pi^0$  (“ $\pi^0$  misid”) and the production of  $\Delta$  baryons which then radiatively decay (“ $\Delta \rightarrow N\gamma$ ”). A test of these NC backgrounds in a measurement with different systematic errors would be quite valuable to firmly establish the oscillation excess.

MiniBooNE can perform this test by detecting neutrons associated with oscillation candidate events. In brief, at low  $E_\nu^{QE}$ , true CC oscillation events (Fig. 3a) should contain neutrons in less than 10% of the events while the NC backgrounds (Figs. 3b,3c) should contain neutrons in  $\approx 50\%$  of the events.

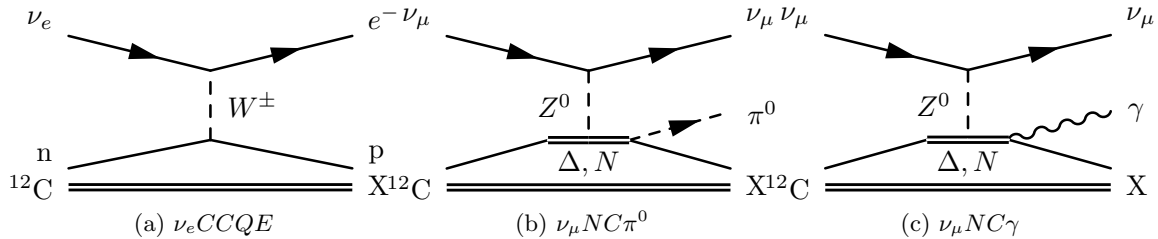


Figure 3: Diagrams of signal (a) and background (b,c) neutrino oscillation candidate events.

Note that  $E_\nu^{QE}$  is the reconstructed neutrino energy using the assumption of neutrino quasielastic scattering from a neutron. This quantity should be a good estimate for the actual neutrino energy in true CC oscillation events (excepting possible nuclear effects, Sec. 3.4). However, because of the large missing energy in NC events, the actual neutrino energy is, on average, much higher than  $E_\nu^{QE}$  for NC background events. So, in a first approximation, the NC backgrounds will contain more final state neutrons because the events are from higher true neutrino energy. More energy is transferred to the nucleus which causes more neutron production as compared to the CC signal in which the true neutrino energy is lower and (neglecting final state interactions) produces a single proton.

In practice, we would rerun the MiniBooNE oscillation search in neutrino mode after the addition of scintillator in order to enable neutron detection. Oscillation candidates would be selected with the same strategy as the original search. From this sample, we would search for neutron capture events and measure the neutron fraction which would test the NC background estimates. An important feature of this measurement is that the neutron fraction may be “calibrated” for the oscillation search via separate MiniBooNE  $\nu_\mu$  CCQE and  $\nu_\mu$  NC $\pi^0$  measurements which greatly reduces errors from any nuclear model uncertainties. A quantitative study that includes a more

complete nuclear physics model, estimates of final-state interactions, detector efficiency, and an estimate of sensitivity is presented in Section 5.

### 3.2 Proton to neutron ratio in NC elastic events

The NC neutrino-nucleon elastic scattering (NC elastic) interaction,  $\nu N \rightarrow \nu N$ , is sensitive to the isoscalar-axial structure of the nucleon [7], so will be sensitive to the effects of strange-quark contributions to the nucleon spin ( $\Delta s$ ). Therefore, the right type of measurement of NC elastic scattering would contribute substantially to the nucleon spin puzzle, an area of continued interest and effort (e.g. [8]). This measurement of NC elastic scattering has not yet been realized.

MiniBooNE has made the most accurate measurement to date of the differential cross section for  $\nu N \rightarrow \nu N$  [9] and the analysis for the  $\bar{\nu} N \rightarrow \bar{\nu} N$  process is almost complete [10]. While these are valuable measurements to help with understanding of neutrino-nucleon scattering, they are not sensitive to  $\Delta s$  because the acceptance of MiniBooNE is approximately equal for neutrons and protons. The  $\nu p \rightarrow \nu p$  process is sensitive to  $\Delta s$  with the opposite sign as  $\nu n \rightarrow \nu n$  and any strange quark effects cancel in the existing MiniBooNE measurement.

This situation changes abruptly with the addition of neutron-capture tagging. In that case, the neutrons and protons can be separately identified and the neutron/proton ratio,

$$R(p/n) = \frac{\sigma(\nu p \rightarrow \nu p)}{\sigma(\nu n \rightarrow \nu n)}, \quad (1)$$

is quite sensitive to  $\Delta s$  [7]. Based on previous studies [11], a rough estimate is that a 10% measurement of  $R(p/n)$  should result in an error of  $\approx 0.05$  uncertainty on  $\Delta s$ . It should be realized that the recent results from MiniBooNE on the unexpectedly large CCQE cross section [12] may call into question the theoretical uncertainty involved in extracting  $\Delta s$  from  $R(p/n)$ . If there are multinucleon correlations contributing substantially to NC elastic scattering, it may not be clear how that affects the extraction of  $\Delta s$ . Regardless, a 10% measurement of  $R(p/n)$  will be a valuable constraint and will spur more theoretical investigation.

### 3.3 A measurement of $\nu_\mu \ ^{12}\text{C} \rightarrow \mu^- \ ^{12}\text{N}_{\text{g.s.}}$

The reaction  $\nu_\mu \ ^{12}\text{C} \rightarrow \mu^- \ ^{12}\text{N}_{\text{g.s.}}$  is an interesting reaction to study with a scintillator-enhanced MiniBooNE for several reasons. It comes with a distinctive tag from the  $\beta$ -decay of the  $^{12}\text{N}_{\text{g.s.}}$  with endpoint energy of 16.3 MeV and lifetime of 15.9 ms. This addition of scintillator to MiniBooNE will allow for high efficiency and better reconstruction of the  $\beta$ -decay. Since it is an exclusive reaction, the theoretical cross section can be calculated to  $\approx 2\%$  very near threshold [13]. It was measured by LSND for both  $\nu_\mu$  and  $\nu_e$  [13, 14] and by KARMEN for  $\nu_e$  [15] to agree with theory to within experimental errors. A measurement by MiniBooNE of this theoretically well-known reaction would enable a test of the low-energy neutrino flux which could better constrain the low-energy oscillation excess.

The event signature is quite distinct. The low-energy prompt  $\mu^-$  and subsequent decay  $e^-$  would be detected with the usual techniques employed for  $\nu_\mu$  CCQE events combined with a requirement for a detected  $\beta$ -decay candidate. With the addition of scintillator to make 2.2 MeV  $\gamma$  visible, the efficiency for detecting the 16.3 MeV-endpoint  $\beta$  will be quite high.

The challenge is that the fraction of the total  $\nu_\mu$  scattering events that interact via  $\nu_\mu \ ^{12}\text{C} \rightarrow \mu^- \ ^{12}\text{N}_{\text{g.s.}}$  is small. In the lowest energy bin at  $E_\nu \approx 250$  MeV, the cross section is about 4% of the  $\nu_\mu$  CCQE cross section, falling to about 0.5% by  $E_\nu \approx 400$  MeV [16]. However, with the data sample proposed here the total  $\nu_\mu$  event sample will be large, the  $^{12}\text{N}_{\text{g.s.}}$  signature quite distinct, and an analysis will be worth the effort.

### 3.4 A test of the QE assumption in neutrino energy reconstruction

MiniBooNE has reported absolutely normalized cross sections for various  $\nu_\mu$ -carbon processes including  $\nu_\mu$  CCQE [12],  $\text{CC}\pi^+$  [17],  $\text{CC}\pi^0$  [18], NC elastic [9], and  $\text{NC}\pi^0$  [19]. They all show a 30-40% larger cross section than predicted in previously existing models (e.g. [20]). One emerging idea is that two-nucleon correlations in carbon are contributing significantly to the interaction cross section [21, 22]. If this is the correct explanation for the extra strength in these neutrino interactions, then it could also have a significant effect on the reconstructed neutrino energy in oscillation events,  $E_\nu^{QE}$ , which assumes quasielastic scattering from single nucleons within carbon [23]. In short, the reconstructed neutrino energy may be incorrect in a large fraction of the oscillation events leading to incorrect conclusions about the resulting fits to oscillation models.

The addition of scintillator will allow this idea to be experimentally tested. With the scintillator addition proposed here, the detector response to final state nucleons in a typical CCQE event will be increased by about a factor of five. This scintillation light is a measure of the total energy in the event ( $E_\nu^{total}$ ) as opposed to that reconstructed from just the lepton track,  $E_\nu^{QE}$ . A comparison of  $E_\nu^{QE}$  with  $E_\nu^{total}$  will allow further insight into the two-nucleon correlation issue in general and, specifically, into its relevance to the low-energy oscillation excess.



## 4 Increasing scintillation in MiniBooNE

In order to execute the main goal of a NC/CC test of the oscillation excess, the detector light output response to neutron captures in MiniBooNE must be increased. This can be accomplished by adding a few hundred parts per million of a scintillator such as butyl-PBD or PPO to the MiniBooNE mineral oil. The resulting level of scintillation will provide a distinct signature of neutron capture. This technique was demonstrated and used by the LSND experiment [24] to search for  $\bar{\nu}_e$  appearance oscillations via inverse  $\beta$ -decay with coincident neutron signal.

When a fast neutron of up to a few hundred MeV is produced by a neutrino interaction in mineral oil ( $\text{CH}_2$ ), it rapidly loses energy by elastic and inelastic collisions with the mineral oil until it is reduced to thermal energies (i.e. “thermalizes”). This thermal neutron will capture on hydrogen 99.5% of the time and on carbon the remaining times with a total characteristic lifetime of 186  $\mu\text{s}$  for mineral oil. The hydrogen capture ( $np \rightarrow d\gamma$ ) yields a 2.2 MeV  $\gamma$ , while the  $^{12}\text{C}$  capture emits a 5 MeV  $\gamma$ .

In addition to allowing for neutron identification (i.e. “n-tagging”), increasing the scintillation light in MiniBooNE will also allow for better sensitivity to the sub-Cerenkov threshold events (e.g. nucleons) in addition to the super-Cerenkov leptons.

### 4.1 Neutron capture

By measuring the energy, position, and time of the event, a selection criteria can be formed which will select n-capture events that are correlated with the primary neutrino event with high efficiency yet reject accidental events. The LSND experiment used the n-capture technique to select  $\bar{\nu}_e p \rightarrow e^+ n$  events via detection of the prompt  $e^+$  signal in coincidence with the delayed 2.2 MeV photon from neutron capture. A neutron likelihood can be formed with the PMT hit multiplicity, prompt-delayed capture distance, and timing distribution, and it was able to achieve a 51% detection efficiency for correlated n-capture events while only being susceptible to a 1.2% accidental probability.

The average PMT multiplicity from a 2.2 MeV  $\gamma$  was 35 PMT hits in the LSND experiment. As MiniBooNE and LSND are comparably sized detectors with similar readout PMTs, the same efficiency and accidental rate suppression can be achieved by raising the MiniBooNE scintillation to yield the same PMT multiplicity for 2.2 MeV  $\gamma$ . LSND, with 25% photocathode coverage, was able to achieve this light yield with 30 mg of butyl-PBD per liter of mineral oil. MiniBooNE has an 11% photocathode coverage, and this requires a higher amount of scintillator to achieve similar performance.

### 4.2 Scintillation light in MiniBooNE, currently

Sub-Cerenkov-threshold particles can produce some light in the current MiniBooNE configuration with “pure” mineral oil. This occurs because of aromatic benzene-like impurities in the MiniBooNE mineral oil, and the light output from these has been characterized in a variety of benchtop and in-situ tests [25, 26, 27]. The various tests are in reasonable agreement and have enabled the scintillation and related fluorescence to be characterized and coded into the MiniBooNE detector Monte Carlo (MC) simulation of the optical model. The main result that can be used to benchmark the well-characterized MiniBooNE oil is that it has a scintillation strength of 32 visible photons emitted per MeV of energy deposit at a wavelength peak of 350 nm, with width  $\sigma = 25$  nm, and a decay time of 34 ns [27].

The results of these scintillation tests have been folded into a complete, optical-photon model that accounts for absorption, re-emission, and various scattering processes, and well-describes the

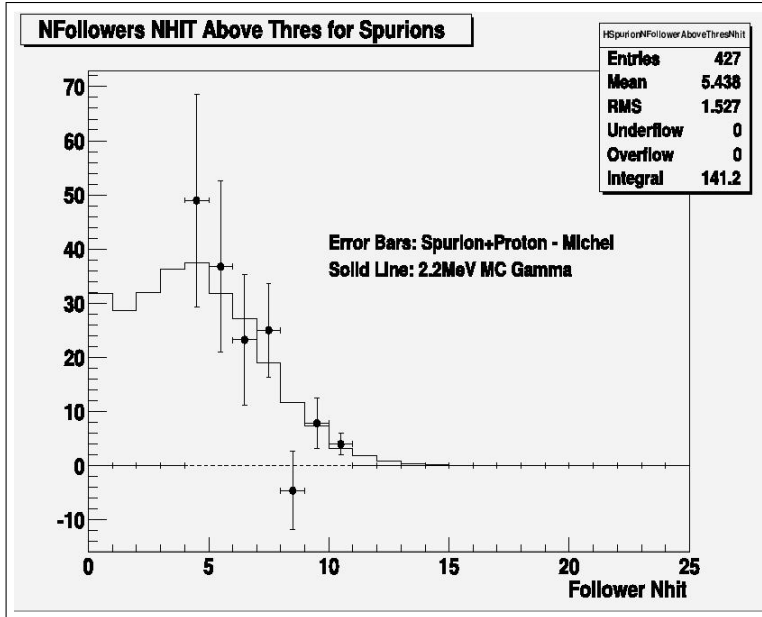


Figure 4: PMT multiplicity distribution from neutron-capture candidate events in an 2004 data study [28]. The data points are shown with error bars after subtraction of random coincidence rate. There is no data below 4 hits because of the trigger threshold. The MC prediction is shown as solid histogram. “Spurion” was a whimsical name given to neutron-capture candidates.

MiniBooNE data. The optical-photon model has been used to predict the current MiniBooNE response (undoped with additional scintillators) to 2.2 MeV  $\gamma$ , and it predicts a multiplicity of approximately 5 PMT hits with about 80% of the light in the directed Cerenkov cone. The remaining 20% of light is due to both isotropic scintillation and the isotropic re-emission of scattered UV Cerenkov light. These results have been verified in a study with MiniBooNE data in 2004 [28] to determine the feasibility of adding a neutron-capture trigger at that time. Figure 4 shows the PMT multiplicity distribution for neutron-capture candidate events (“follower” events) derived from this study. This shows that the MC correctly simulates the current level of scintillation and response to 2.2 MeV n-capture events, and that the response is too low to conduct a neutron search with the current scintillation level (nominally undoped, less the fluorescent impurities).

### 4.3 Simulations of increased scintillation light

We first assess how much light must be produced by a given scintillator before determining the amount of scintillator required. Using the MiniBooNE detector MC, the total scintillation fraction can be increased, and the PMT multiplicity simulated for 2.2 MeV n-capture  $\gamma$ . As the scintillation level is increased by a scaling factor  $k$ , the total isotropic response (not in the prompt, directed Cerenkov light cone) increases faster than  $k$  because the scintillator absorbs Cerenkov light in the UV (not detected by the PMTs) and shifts it into the PMT wavelength sensitivity range. This additional contribution is isotropically re-emitted and is then detected by the PMTs.

Initial light output tests were performed with a naive scintillation model by scaling the 350 nm light emitted by the current fluors present in the MiniBooNE oil. A more sophisticated model was developed that utilized a fluor model more appropriate for butyl-PPD, and this model was based upon the emission and absorption spectra for butyl-PBD which are shown with the PMT quantum efficiency (QE) in Fig. 5. A fluor such a butyl-PBD is more efficient at increasing the scintillation

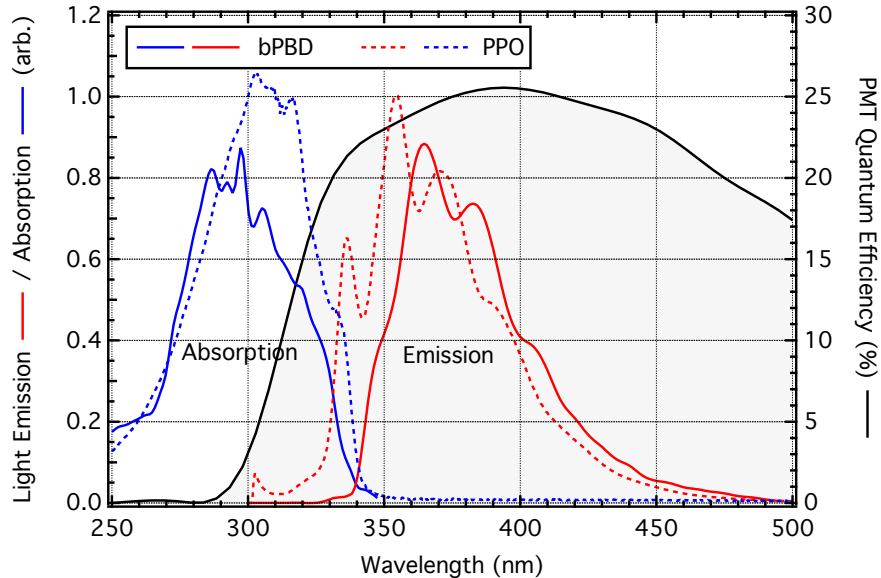


Figure 5: The absorption and emission spectra of butyl-PBD and PPO with the MiniBooNE PMT quantum efficiency overlaid on the right.

compared to the current fluors in the MiniBooNE oil because the emission spectrum has a longer average wavelength for which the attenuation length of the mineral oil is longer and the PMT QE is higher. Also, butyl-PBD has comparable fast and slow scintillation components (2 ns and 20 ns, respectively) in contrast to the current MiniBooNE fluors which contain just a slow component (34 ns). The fast scintillation component significantly improves the reconstruction of the n-capture position reconstruction as will be seen below in Sec. 4.4.

The results from the MC studies are summarized in Fig. 6. Note that the efficiency for finding events over threshold (PMT multiplicity) of 10 hits increases with the scintillation multiplier as does the average PMT multiplicity. A scintillation multiplier of 1 represent no additional scintillation beyond that of the current MiniBooNE fluors in mineral oil (32 photons / MeV). Also note that the butyl-PBD model with a scintillation multiplier of 15 is equivalent to the naive model at about a value of 22 because butyl-PBD has a more optimal overlap of its emission spectrum with the PMT QE and there is a longer attenuation length of mineral oil at these wavelengths. The detection efficiency and PMT multiplicity results for butyl-PBD lead to the conclusion that a multiplication factor of 15 times the current MiniBooNE value is sufficient to reconstruct the 2.2 MeV n-capture  $\gamma$ .

#### 4.4 Event reconstruction

Based on the MC studies of increased scintillation light in n-capture events, an increase of the scintillation strength by a factor of 15 with butyl-PBD (or similar) should be adequate. Further studies were performed using the existing MiniBooNE reconstruction apparatus to determine how well 2.2 MeV  $\gamma$  and higher energy electrons are reconstructed with their increased scintillation light.

Low-energy events such as 2.2 MeV  $\gamma$  are reconstructed using PMT charge and time information. For position reconstruction, the time information is the most critical as the time of arrival at each tube allows the position to be determined. It is crucial to have a scintillator with a fast time component or the position information is degraded. This is especially true with low-light

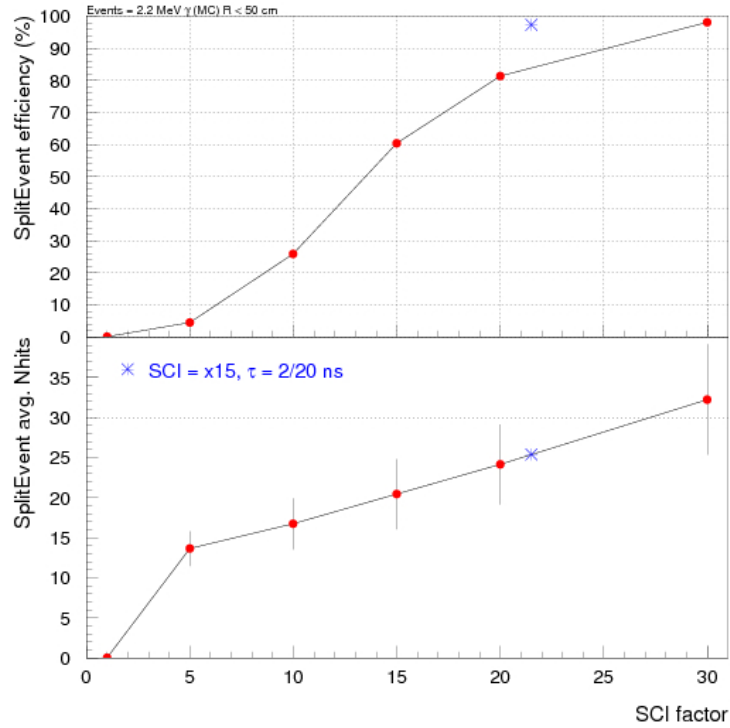


Figure 6: Neutron capture (2.2 MeV  $\gamma$ ) event detection efficiency (top) and the average PMT multiplicity distribution (bottom) is shown as a function of scintillation strength multiplier (SCI factor). The red points are from the naive scintillation model where the current 350 nm MiniBooNE mineral oil emission is scaled from current value. The blue point is for the butyl-PBD model at scintillation strength of 15 times the current MiniBooNE mineral oil and with light output equivalent to the naive scintillation model with a strength multiplier of about 22.

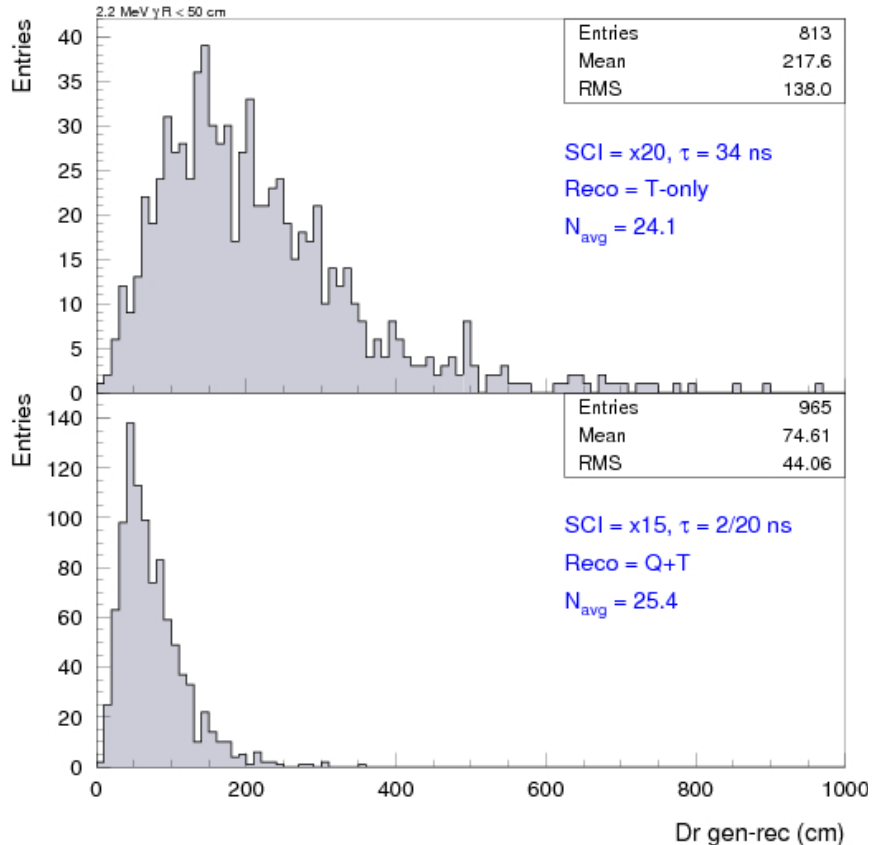


Figure 7: Position resolution of simulated 2.2 MeV  $\gamma$  events for the naive scintillation model (top) compared to that for the butyl-PBD model (bottom).

events where the PMTs are typically detecting an average of one photoelectron. These effects can be seen in Fig. 7 where the position resolution for 2.2 MeV  $\gamma$  is plotted for both the naive and butyl-PBD scintillation models, using new reconstruction algorithms developed specifically for this task. The butyl-PBD model with a fast scintillation component of 2 ns results in improved position reconstruction of  $\approx 75$  cm. This is comparable to that achieved in the LSND n-capture reconstruction and, therefore, should yield similar n-capture efficiency and accidental background rejection.

Adequate reconstruction of n-capture events is only part of the reconstruction battle. This increased level of scintillation light must not degrade the electron reconstruction which is crucial for an oscillation analysis. This was studied by generating electron events using the detector MC with the butyl-PBD scintillation model and then reconstructing these events using the current MiniBooNE algorithms. This was first tested with 50 MeV electrons. The Cerenkov cone is still readily located within the increased scintillation light as can be seen in Fig. 8 where the angular distribution of the light around the reconstructed electron direction is plotted. The level of isotropic light is increased by about a factor of 15 as expected, but the higher level of directed light in the Cerenkov cone is still quite obvious.

The reconstruction of higher energy electrons has also been studied. In order to obtain the optimum reconstruction of neutrino events, the PMT charge and time likelihoods will need to be redetermined for the new scintillator mixtures. This has not been addressed fully at this time.

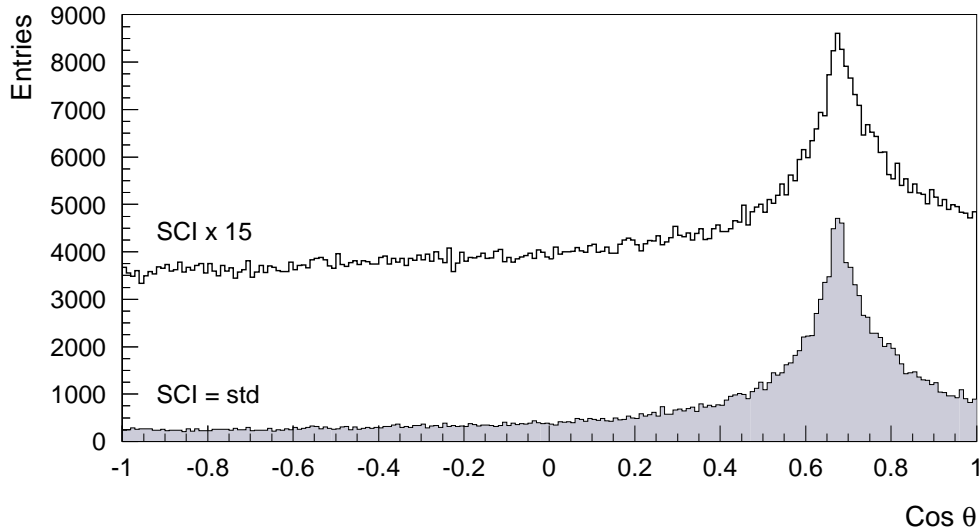


Figure 8: Angular distribution of light around the reconstructed direction of 50 MeV electrons for the standard (current) scintillation model compared to the butyl-PBD model.

However, a few steps in that direction have been taken and these intermediate results allow some conclusions to be made. First some details need to be explained.

MiniBooNE has several levels of reconstruction, the first “SFitter” assumes a point like model for the lepton track. The second “RFitter” contains an extended track model [29] and was used for the particle identification (PID) in the main oscillation analysis but is very sensitive to tuning which has not yet been performed. The SFitter has a more complex PID algorithm but is less sensitive to tuning. Results from applying these reconstruction algorithms to the simulated 100-600 MeV electrons are shown in Fig. 9. The SFitter and RFitter results are shown with the standard (current) scintillation model. The SFitter was run with no modifications to the underlying likelihoods and then with only a minor adjustment to the energy scale. There are a few things to note in this plot. First, the untuned SFitter with increased scintillation returns degraded resolution values across the energy range. This is expected as the underlying parameters of the fit are incorrect in this case. However, the SFitter with minor modifications actually has better position resolution than the standard case. It approaches the standard value at higher energy for angular resolution. The performance of the untuned RFitter with increased scintillation is off the scale in Fig. 9.

The conclusions from these studies at this time are that simple changes to the SFitter recover resolution to the standard level after a minor change to adjust for the stronger scintillation light. We expect to improve this for the SFitter with proper tuning of the time likelihoods and underlying optical model. From the behavior of the SFitter, we expect to recover the good resolution for the RFitter after the required retuning of the algorithm.

The results of these studies indicate that an increase of scintillation light with a butyl-PBD type dopant by about a factor of 15 is sufficient for the desired n-capture reconstruction accuracy. In the studies to date, this level of increased scintillation light indicates that the electron reconstruction should not suffer – at least for energies below 600 MeV.

If electrons can be reconstructed sufficiently, it seems reasonable to assume that  $\pi^0$ s and  $\mu$ s may also be reconstructed with accuracy as in existing analyses. However, that has not yet been shown conclusively and is subject of current work. It is an important question.

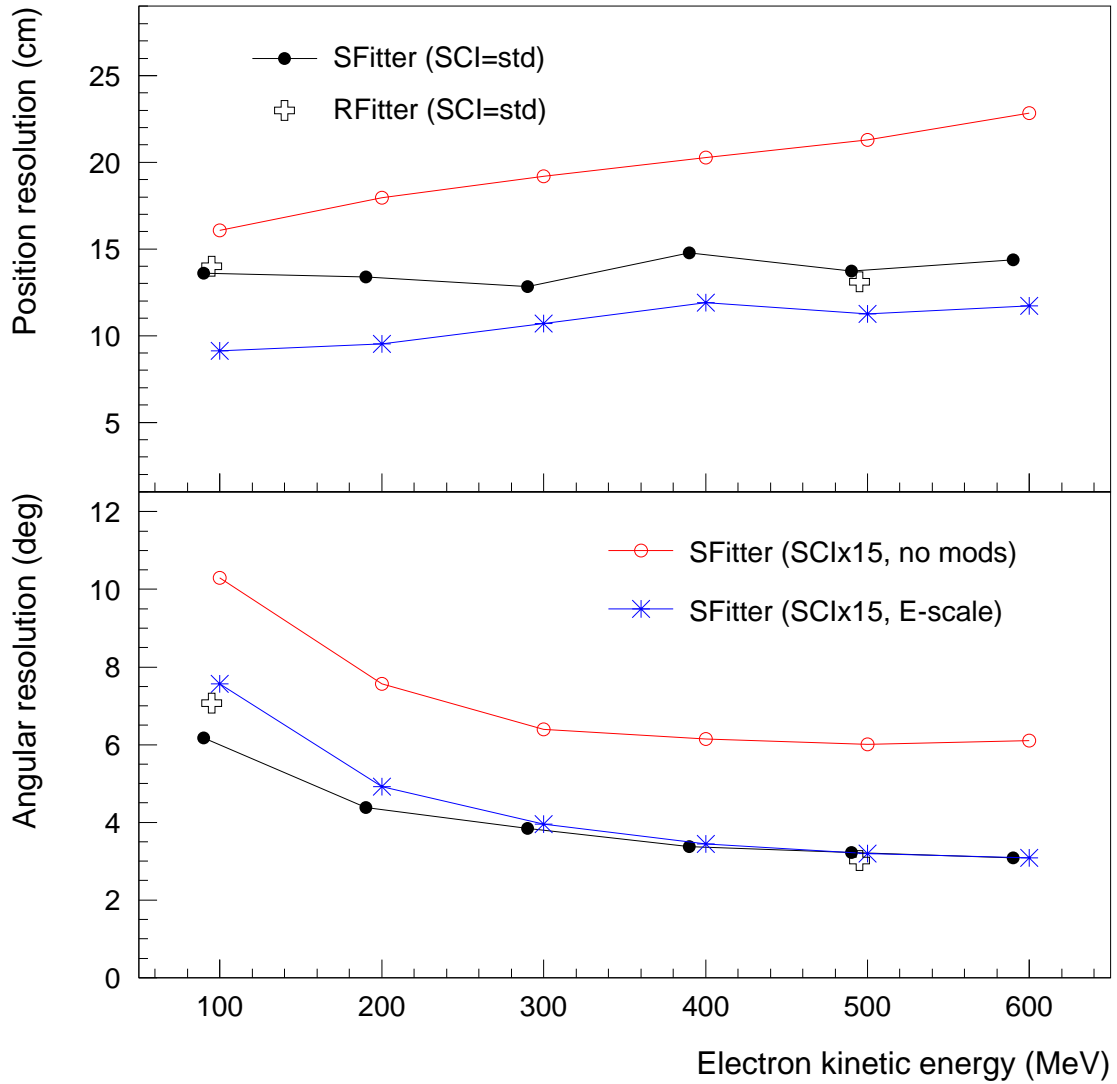


Figure 9: Position (top) and angular (bottom) resolution obtained with the MiniBooNE reconstruction “SFitter” and “RFitter” algorithms for 100-600 MeV electrons with both the standard (current) scintillation model and a butyl-PBD model. The Rfitter was run at only 100 and 500 MeV.

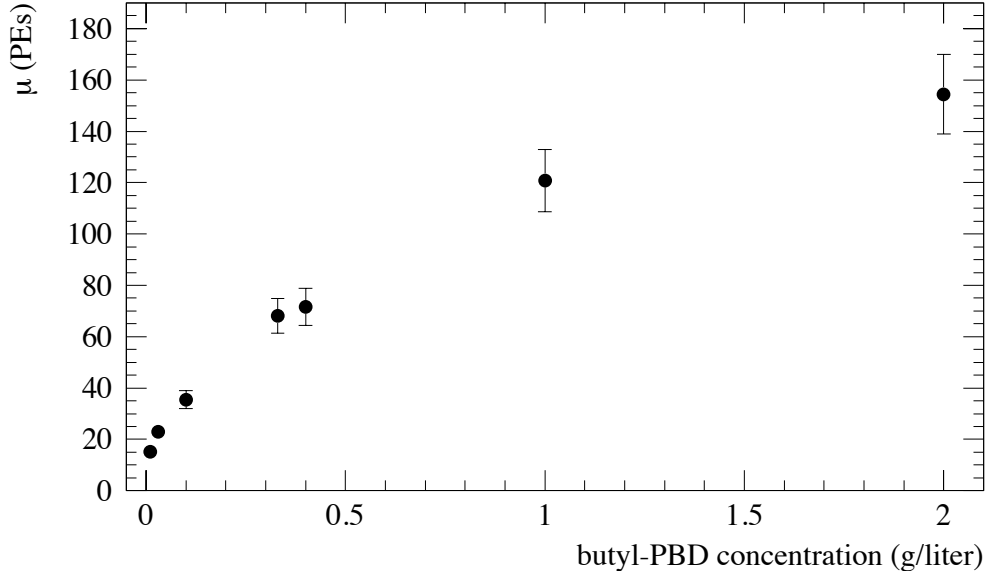


Figure 10: MiniBooNE tests on light level vs. concentration of butyl-PBD [30]. The vertical scale is number of photoelectrons (PE) produced with that particular apparatus.

#### 4.5 Determination of the scintillator cocktail

From the studies in the preceding sections, we have determined that we should add an amount of scintillator with absorption/emission spectrum and lifetime of butyl-PBD to obtain a light yield of 15 times that the current level in MiniBooNE.

To determine the scintillator concentration that will produce this light level, we have examined data collected during MiniBooNE oil tests in 2001-2002 together with recent tests. In 2001-2002, the level of scintillation in candidate mineral oils for MiniBooNE was measured at the Indiana University Cyclotron Facility proton beam [30]. This beam was ideal for these tests as the 200 MeV proton beam is below the Cerenkov production threshold, and a direct measurement of the isotropic scintillation light could be isolated. While the tests focused on the scintillation from pure mineral oil, several scintillators were tested with the idea that a slight amount of scintillator could be beneficial for MiniBooNE particle identification. The tests with butyl-PBD are shown in Fig 10. In separate tests, it was determined that scintillation from pure MiniBooNE mineral oil produced 5 photoelectrons with the same experimental setup. Therefore, in order to produce a factor of 15 more light than pure MiniBooNE mineral oil (Sec. 4.3), approximately 0.3 g/l of butyl-PBD is desired. Similar tests of butyl-PBD were carried out in service of LSND [31] and are consistent with the MiniBooNE results.

In the process of considering butyl-PBD<sup>1</sup> as a candidate scintillator, PPO<sup>2</sup> was identified as another possibility. As can be seen in Fig. 5 the absorption / emission spectra are quite similar between butyl-PBD and PPO. In addition, the light output at a given concentration of PPO in mineral oil is about the same as butyl-PBD, and the characteristic emission times are about the same with a fast component around 2 ns [32]. In preliminary investigations about price, PPO looks to be about 1/4 of the price per kg of butyl-PBD.

In order to investigate PPO further and to verify the old results on butyl-PBD, the test setup

<sup>1</sup>Butyl-PBD is a synonym for 2-(4-tert-Butylphenyl)-5-(4-biphenyl)-1,3,4-oxadiazole, CAS Number 15082-28-7

<sup>2</sup>PPO is a synonym for 2,5-Diphenyloxazole, CAS Number 92-71-7



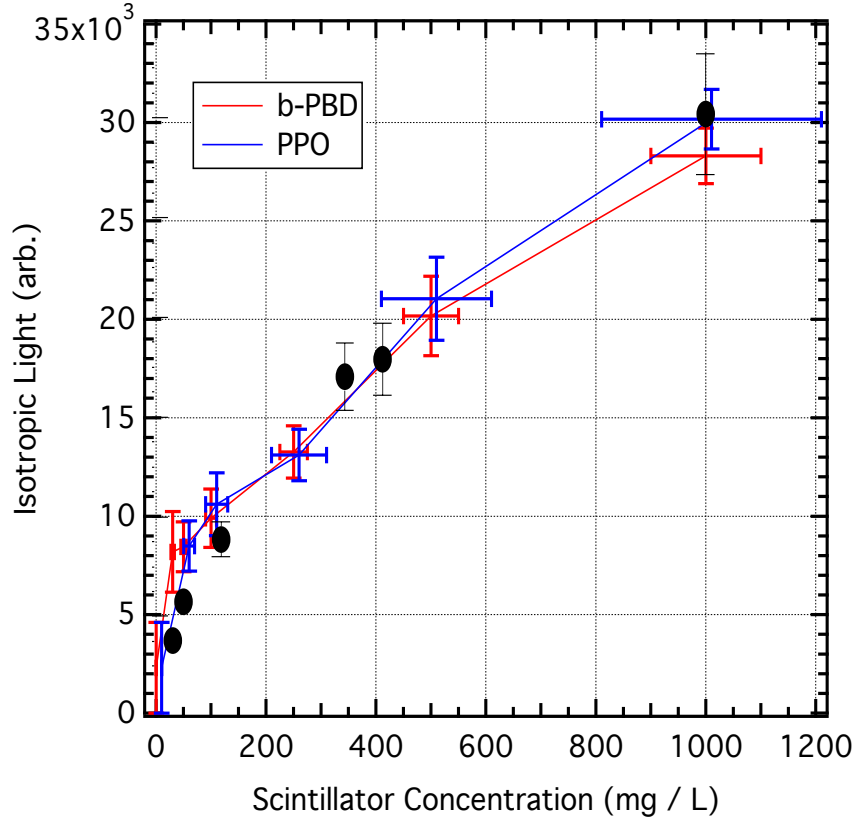


Figure 11: Recent tests of isotropic light output from butyl-PBD and PPO in mineral oil as a function of scintillator concentration. The recent lab tests are shown as red and blue points. The data taken from early mineral oil tests with butyl-PBD [30] are shown as black points and are overlaid.

from the 2001-2002 IUCF tests was modified. Instead of operating in the 200 MeV proton beam, the test setup utilized a strong, collimated  $^{60}\text{Co}$   $\gamma$  source with the original oil test apparatus. The light output of various concentrations of butyl-PBD and PPO in mineral oil were tested, and the results are shown in Fig. 11. From these tests it was determined that the light output from butyl-PBD and PPO at a given concentration are the same. The data from 2001-2002 IUCF tests [30] on butyl-PBD are overlaid on the plot with an arbitrary matching of scale as the light collection efficiency in the current setup is not absolutely calibrated. However, the behavior with scintillator concentration is the same between the different tests. If the old data is used to set the scale, then our current tests indicate that PPO has the same light output as butyl-PPD and a concentration of 0.3 g/l of PPO will yield a factor of 15 light increase in the MiniBooNE mineral oil.

## 5 Simulated oscillation analysis

In this section we report the results of a simulated analysis to determine the sensitivity of an oscillation search with NC/CC identification via identification of n-capture events. The method assumes that the oscillation search will be repeated with a new data set, after adding scintillator to MiniBooNE. It also assumes that a candidate oscillation sample is obtained using the same particle ID strategy and, for this study, that the backgrounds and excess are the same as obtained from the current MiniBooNE results. The neutron-capture analysis is then performed with this simulated oscillation sample.

### 5.1 Measuring the neutron fraction in oscillation candidate events

A simulated measurement of the neutron fraction in oscillation candidate events was performed using the current MiniBooNE neutrino oscillation data set and is summarized in Fig. 12. Figure 12(top) shows the  $E_\nu^{QE}$  distribution of the simulated data events along with the background predictions and is the same as Fig. 1(top) excepting that unnormalized events plotted are shown and the backgrounds have been regrouped into four categories:  $\nu_e$  CC,  $\nu_\mu$  CC,  $\nu_\mu$  NC, and dirt. This study assumes that the systematic and statistical errors will be the same as in the existing MiniBooNE neutrino set which resulted from  $6.5 \times 10^{20}$  POT.

For this study, each of the four backgrounds were modeled to predict the fraction (before n-capture efficiency) of events with an associated neutron. For the  $\nu_\mu$  CC and  $\nu_e$  CC background events, the model assumed that 1% of events in the 250 MeV bin had associated neutrons and rising to 10% at 1 GeV. This low energy behavior is based on a measurement by the LSND experiment [13] of the neutron fraction in  $\nu_\mu$   $^{12}\text{C} \rightarrow \mu^- X$  events at mean  $\nu_\mu$  energy above  $\mu^-$  threshold of 156 MeV. The upper limit comes from an  $^{12}\text{C}(e, e'p)X$  experiment [33] that measured nuclear transparency at an average proton recoil energy of 180 MeV. Note that this model, since it is based on actual measurements from carbon, includes the effects of final state interactions of the nucleons as they exit the nucleus.

For the  $\nu_\mu$  NC events, a neutron fraction of 50% was assumed. This is based on models that predict the dominance of incoherent  $\Delta$  production in both NC $\pi^0$  and NC $\gamma$  production [37, 39] and that  $\Delta$  will decay symmetrically to neutron or proton. The “dirt” background is assumed to be neutron free since it is likely photons that are produced in the material around the MiniBooNE detector tank and escape detection as they travel through the veto. This assumption is not critical since the dirt background is a small fraction of sample. The neutron fraction of the dirt background will be measured in the actual analysis. For the  $\nu_e$  CC oscillation signal, the neutron fraction will be the same as for the  $\nu_e$  CC background described above.

These assumptions will need to be fine tuned with a more complete model. The recent work of Refs. [34]-[39] together with actual measurements of the reaction channels contributing to the backgrounds (Sec. 5.3) will make this possible. The central value of the predicted neutron fraction will actually be somewhat different than 50% due to NC scattering from free protons (in  $\text{CH}_2$ ) and coherent scattering which do not result in neutrons in the final state. However, final-state interactions of neutrons in NC interactions producing additional neutrons, will move the neutron fraction to higher values. These uncertainties are explored by varying the underlying assumptions and is also quantified in following paragraphs.

In addition to a model for the fraction of neutrons in the signal and background channels, a neutron efficiency was needed as input. This was set to be the same as for the LSND experiment, 50% [6], since the detection method and scintillation light level will be similar. One other input required for this study is the probability for accidental neutrons passing the n-capture cuts. This

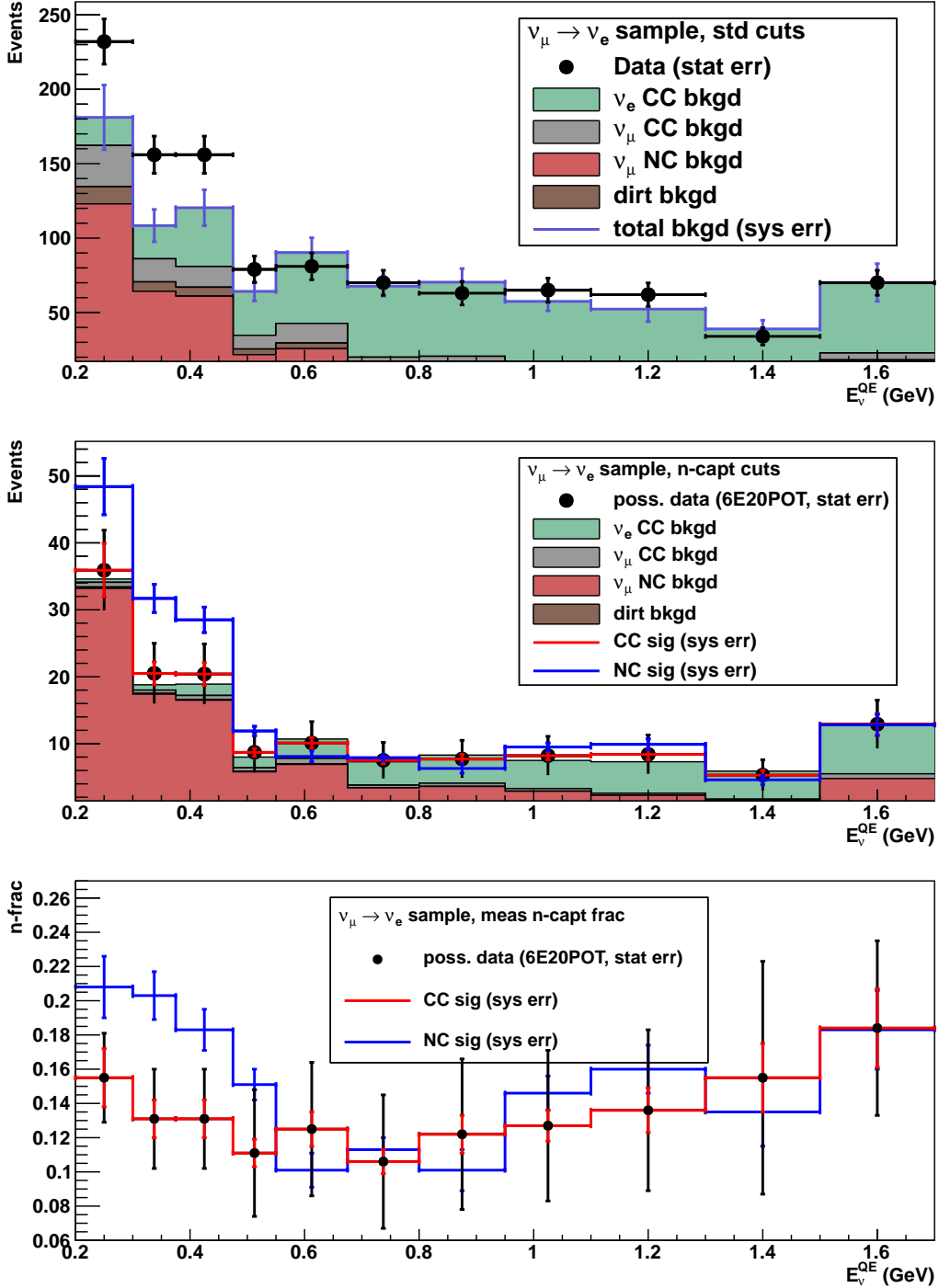


Figure 12: Simulated neutron fraction measurement using the existing MiniBooNE neutrino data set. The  $E_{\nu}^{QE}$  distribution of the current data set is shown in the top plot, the middle plot contains events that have an associated n-capture event, and bottom is the simulated measured neutron fraction. In the middle and top plots, the red (blue) curve is the prediction if the excess is due to CC signal (NC background) with systematic errors and the data points are drawn using the CC signal hypothesis with statistical errors.

was set to be 2%, again the same as for the LSND experiment.

The systematic errors identified and quantified in this study are from the following uncertainties:

- Predicted NC, CC, and dirt backgrounds. The values for the associated uncertainties are extracted from the MiniBooNE constrained oscillation fit and are 10-12% in the lowest energy bins where the NC backgrounds dominate.
- Predicted NC and CC neutron fractions. These errors are set to 5% relative for both NC and CC channels.
- Assumed n-capture efficiency. Set to 1% uncertainty as it will be the same value and completely correlated between the background and signal assumptions.

When these simulated n-capture cuts are applied to the study sample of Fig. 12(top), the event distribution shown in Fig. 12(middle) results. Since the CC backgrounds contain very few neutrons they are greatly reduced in the resulting sample. The n-capture cuts are effectively an NC selection. The oscillation excess, assumed in this study to be all  $\nu_e$  CC oscillation events, disappears with the neutron requirement. This can be seen as the simulated data distribution is the same as the prediction with the CC signal assumption. On the other hand, if the oscillation excess is instead due to an incorrect calculation of the NC background, the sample will instead show an excess as shown for the NC “signal” in the figure.

This situation is more easily examined in Fig. 12(bottom) where the neutron-fraction distribution is plotted. Again, the data is assumed to have an excess over background due to  $\nu_e$  CC oscillation events so it overlays the CC signal prediction. The NC prediction is significantly above the CC prediction and the two possibilities are quite distinct in the lowest  $E_{\nu}^{QE}$  where the excess appears. In this plot, the total estimated systematic errors are shown on the predictions and the resulting statistical errors on a  $6.5 \times 10^{20}$  POT sample are shown on the simulated data points.

Using this simulated neutron fraction, an oscillation excess significance test was extracted by calculating the separation between the simulated data with the excess assumed to be  $\nu_e$  CC oscillation events (the data points with statistical errors in Fig. 12(bottom)) and the NC prediction (the top histogram in Fig. 12(bottom) with systematic errors). The resulting significance is  $3.5\sigma$  and is limited by statistical error. It has effectively no correlation with the first-stage oscillation result (without n-capture). So, the  $3.5\sigma$  excess can be combined *independently* with the  $3.4\sigma$  neutrino-mode excess (if it is present in this new data set). The combination yields a significance of  $\approx 5\sigma$ .

Another method to quantify these simulated results is a null exclusion test. This was performed by forming a  $\chi^2$  from the simulated data as compared to the null hypothesis (NC prediction). The sum in this test ran over all  $E_{\nu}^{QE}$  in the neutron-fraction distribution of Fig. 12(bottom). The resulting null exclusion probability, if the excess is due to  $\nu_e$  oscillations, is 0.03%.

## 5.2 Variations of study assumptions

The assumptions explained in the previous section were varied in alternate models in order to determine the effect on the resulting significance of the oscillation hypothesis test. These studies are summarized in Table 1.

The top row of Table 1 summarizes the results of the significance study with the assumptions explained in Sec. 5.1 which yields a significance value of  $3.5\sigma$ . Note that this includes the assumption of  $6.5 \times 10^{20}$  POT. The subsequent rows show the values for some possible variations in underlying assumptions. There are a few values of note. If the data sample is reduced to  $2 \times 10^{20}$  POT the significance drops to  $2.2\sigma$ . This is indicative of the fact that this is a statistics limited test. Note

configuration	neutron fraction				difference	n $\sigma$
	NC prediction		fake data			
<b>standard</b>	0.191	$\pm$ 0.008	0.134	$\pm$ 0.015	0.057 $\pm$ 0.016	<b>3.48</b>
4E20POT	0.191	$\pm$ 0.008	0.134	$\pm$ 0.018	0.057 $\pm$ 0.019	2.95
2E20POT	0.191	$\pm$ 0.008	0.134	$\pm$ 0.026	0.057 $\pm$ 0.027	2.16
(bckgnd error) $\times$ 0.5	0.191	$\pm$ 0.005	0.134	$\pm$ 0.015	0.057 $\pm$ 0.015	3.73
(n-capture efficiency)=0.75	0.277	$\pm$ 0.012	0.191	$\pm$ 0.018	0.086 $\pm$ 0.021	4.13
(accidental efficiency) $\times$ 2	0.211	$\pm$ 0.008	0.154	$\pm$ 0.016	0.057 $\pm$ 0.017	3.29
(CC n-fraction) $\times$ 2	0.191	$\pm$ 0.008	0.137	$\pm$ 0.015	0.054 $\pm$ 0.017	3.26
(low-E CC n-fraction)=0.06	0.199	$\pm$ 0.008	0.147	$\pm$ 0.015	0.051 $\pm$ 0.017	3.00
(NC n-fraction error) $\times$ 2	0.191	$\pm$ 0.010	0.134	$\pm$ 0.015	0.057 $\pm$ 0.017	3.31
dirt n-fraction=0.5	0.203	$\pm$ 0.008	0.145	$\pm$ 0.015	0.057 $\pm$ 0.017	3.32
(NC bckgnd) $\times$ 2	0.215	$\pm$ 0.011	0.175	$\pm$ 0.014	0.040 $\pm$ 0.017	2.29
(NC bckgnd) $\times$ 2 + $\infty$ POT	0.215	$\pm$ 0.011	0.175	$\pm$ 0.000	0.040 $\pm$ 0.010	3.81
(NC n-fraction)= 0.42	0.165	$\pm$ 0.006	0.117	$\pm$ 0.014	0.048 $\pm$ 0.015	3.17
$\infty$ POT	0.191	$\pm$ 0.008	0.134	$\pm$ 0.000	0.057 $\pm$ 0.008	7.63

Table 1: Summary of simulated results for a neutron fraction measurement with the oscillation sample. In this study the “NC prediction” is the expected value for neutron fraction with systematic errors in the case if the oscillation excess was all from NC backgrounds. The “fake data” is with the assumption that the oscillation excess is all CC oscillation signal with statistical errors. The top row (“standard”) is with the standard assumptions as explained in Sec. 5.1 and with  $6.5 \times 10^{20}$  POT, and the other rows are variations with the standard configuration plus the change indicated.

that with infinite POT the significance goes to  $> 7\sigma$ . While infinite POT is not possible, it points out that further optimization of cuts may be possible to increase statistics while taking some hit in systematic errors. This will be a subject of future study.

Neglecting the event statistics variations, the significance ranges from approximately  $2.3\sigma$  to  $4.1\sigma$ . The lowest value of  $2.3\sigma$  is from an increase in the size of the NC background by a factor of 2. This may happen if the signal to background ratio in the oscillation sample is not held at the current levels with the new analysis after the addition of scintillator. This is an important point. The addition of scintillator to MiniBooNE must not cause a significant change in the oscillation signal purity.

Another variation to note is that where the neutron fraction of NC events is changed from 50% to 42%. This is the value obtained with consideration of free protons. It does lower the significance slightly as does an increase in the assumed neutron fraction of CC current events. However, the significance in the cases does not drop below  $3\sigma$  and it is expected that consideration of neutron final state effects in carbon will increase this. While these variations in the neutron fraction of events may occur it is important to remember that this will not be an unknown variation. These fractions will be measured in calibration samples as explained in the next section.

### 5.3 Calibration of the neutron fraction in NC and CC events

The MiniBooNE low energy excess has stimulated recent theoretical work in non-oscillation explanations of the data, in particular, that the NC $\gamma$  background has been underestimated [40]-[41]. Indeed, if this background was not correctly estimated in the MiniBooNE oscillation analysis, it could be the explanation of the excess. However, recent theoretical results are actually supporting

the MiniBooNE calculations [37]. A side benefit of this theoretical work is that realistic models for NC processes at these energies ( $E_\nu \approx 100 - 500$  MeV) have been improved and better understood which will help any future experiments working in this area. In addition, these models can be used to better understand the n-fraction in NC events which is crucial for the experiment proposed here. However, an important advantage to the n-capture method is that the neutron fraction from both CC and NC events can be measured with this experiment. This, together with model guidance, will keep systematics on backgrounds quite low.

For CC events, one wants to know, as a function of reconstructed neutrino and, in particular at  $E_\nu \approx 100 - 500$  MeV, the neutron fraction in the reaction  $\nu_e C \rightarrow e^- X$  (Fig. 3a). This has been measured at this energy scale by LSND [13] in the  $\nu_\mu C \rightarrow \mu^- X$  reaction as described earlier. The difference between  $\nu_e$  and  $\nu_\mu$  can be calculated with consideration of the higher energy threshold in the  $\nu_\mu$  reaction. This will also be measured by MiniBooNE via  $\nu_\mu C \rightarrow \mu^- X$  events that contain a neutron, identified with the n-capture signal. It is estimated (and used in the study above) that a 5% systematic error may be obtained.

For NC events, the desired quantity is the neutron fraction for the NC oscillation backgrounds,  $\text{NC}\pi^0$  and  $\text{NC}\gamma$  (Figs. 3b, 3c). The  $\text{NC}\pi^0$  background can be measured via  $\nu_\mu C \rightarrow \pi^0 X$  where the  $\pi^0$  is correctly identified in the detector. This measurement has previously been made by MiniBooNE [42, 19]. The extrapolation to the background  $\text{NC}\pi^0$  events is then performed with the detector simulation and is fairly model independent, depending mainly on  $\pi^0$  kinematics.

The  $\text{NC}\gamma$  background may then be calculated from the radiative decay of the  $\Delta$  with the production rate of the  $\Delta$  constrained by the  $\text{NC}\pi^0$  measurement. The change of the  $\Delta$  width in carbon is taken into account. This was the method used by MiniBooNE in the current analysis and has been vindicated with separate theoretical calculations [40, 41]. It is important to note that if there is an anomalous rate for  $\text{NC}\gamma$ , underestimated by both MiniBooNE and current theories, it is likely to produce neutrons 50% of time. If so, this would show up in the n-capture search and an excess of events after NC cuts would occur, thus finding the underestimated background.

## 6 Implementation

In this section, we explore some details of how to prepare and run MiniBooNE with the addition of scintillator.

### 6.1 Suggested plan for adding scintillator

As of this writing, we plan to add 300 kg of PPO to the  $1 \times 10^6$  liters of MiniBooNE mineral oil (300 mg/l). A preliminary price quote for PPO from the supplier to NOvA is \$250/kg or \$75k for scintillator. The solubility of PPO will allow us to add the entire 300 kg to the MiniBooNE 10 kl overflow and then introduce that into the main volume by recirculation. However, it would be prudent to do this addition in at least two steps by taking the concentration to about 50% of the desired amount and monitoring detector response with cosmic muons and muon-decay electrons. We may do recirculation without the addition of scintillator as a first step, as the MiniBooNE oil has not been recirculated since commissioning in 2002.

### 6.2 Detector changes

Our base plan for running with scintillator is only to add scintillator with no other changes. New readout electronics could be considered, but are not required for the physics goals set here. The current rate of PMT and failures extrapolated for a 3-year run is not a problem. We estimate that the rate of electronics failures over that time period will be covered with our current supply of spares. There will likely be some changes to the computing infrastructure to keep up with hardware failures and security concerns, but an “as-needed” approach is our current plan.

### 6.3 Run plan

As shown in Sec. 5, the neutron fraction measurement for oscillation candidates is statistics limited and  $6.5 \times 10^{20}$  POT is required for our current desired accuracy. When the MicroBooNE experiment is running, our assumption is that  $2 \times 10^{20}$  POT/year will be delivered to the Booster Neutrino Beamline (BNB). This sets a 3-year duration for the proposed scintillator phase of MiniBooNE. Preparation for running only requires the addition of scintillator (along with modest detector maintenance), which we estimate will require about 3 months with no beam requirement. If approvals and funding can be obtained reasonably quickly, we estimate that we could be ready to add scintillator by the end of 2013.

### 6.4 Future Work

There are several tasks and milestones to be done before the MiniBooNE collaboration is completely prepared to go forward with adding scintillator. Probably the most important task is to show that the signal to background ratio in the oscillation search is not damaged by the addition of scintillator. The results on electron reconstruction shown here are favorable evidence that this can be accomplished and the LSND was able to do such a reconstruction, albeit at lower energies. However, the definitive test is to also show that particle identification of  $e$ ,  $\mu$ ,  $\pi^0$  is sufficient to repeat the  $\nu_e$  appearance search with adequate background rejection. Work on this is ongoing.

In addition, there are other tasks related to adding scintillator such as:

- adjustment of the MC simulation to account for the new light production mechanism,
- additional light output tests, perhaps in 200 MeV proton beam,

- light attenuation length tests,
- material compatibility tests,
- scintillator procurement plan and price estimates, and
- detailed scintillator mixing and oil recirculation plan.

Work on these tasks is currently underway.



## 7 Conclusions and request

The addition of 300 mg/l of scintillator to the existing MiniBooNE mineral oil will allow for the detection and reconstruction of 2.2 MeV  $\gamma$  from neutron-capture. CC oscillation signal events should have an associated neutron in less than 10% of events in contrast to NC background events in which  $\approx 50\%$  have neutrons. The neutron-capture rate for both of these event types can be separately measured in MiniBooNE, thus eliminating dependence on neutron production model calculations. Therefore, a measurement of neutron-capture in oscillation events measures the NC backgrounds.

A measurement of the neutron-fraction in a new appearance oscillation search with MiniBooNE will increase the significance of the oscillation excess, if it maintains in the new data set, to  $\approx 5\sigma$ . In practice, the  $\nu_e$  appearance search will be conducted again after the introduction of scintillator. With  $6.5 \times 10^{20}$  POT, the results of this search (before neutron capture cuts) should have similar sensitivity as existing search but with different systematic errors. Combining this with the neutron capture analysis will raise the sensitivity to the  $5\sigma$  level, perhaps better, depending on final systematics.

This new phase of MiniBooNE would enable additional important studies such as the spin structure of nucleon ( $\Delta s$ ) via NC elastic scattering, a low-energy measurement of the neutrino flux via the  $\nu_\mu \ ^{12}\text{C} \rightarrow \mu^- \ ^{12}\text{N}_{\text{g.s.}}$  reaction, and a test of the quasielastic assumption in neutrino energy reconstruction. This effort will provide training for Ph.D. students and postdocs and will yield important, highly-cited results over the next 5 years for a modest cost.

*This program of measurements requires approximately  $6.5 \times 10^{20}$  protons on target delivered to MiniBooNE and can begin in early 2014. We are requesting support of this concept to enable the collaboration to plan the experiment and analysis in more detail with the goal of submitting a full proposal for the experiment in mid-2013.*

## References

- [1] A. A. Aguilar-Arevalo *et al.* [MiniBooNE Collaboration], Phys. Rev. Lett. **98**, 231801 (2007) [arXiv:0704.1500 [hep-ex]].
- [2] A. A. Aguilar-Arevalo *et al.* [MiniBooNE Collaboration], Phys. Rev. Lett. **102**, 101802 (2009) [arXiv:0812.2243 [hep-ex]].
- [3] A. A. Aguilar-Arevalo *et al.* [MiniBooNE Collaboration], Phys. Rev. Lett. **103**, 111801 (2009) [arXiv:0904.1958 [hep-ex]].
- [4] A. A. Aguilar-Arevalo *et al.* [MiniBooNE Collaboration], Phys. Rev. Lett. **105**, 181801 (2010) [arXiv:1007.1150 [hep-ex]].
- [5] A. A. Aguilar-Arevalo *et al.* [MiniBooNE Collaboration], arXiv:1207.4809 [hep-ex].
- [6] A. Aguilar-Arevalo *et al.* [LSND Collaboration], Phys. Rev. D **64**, 112007 (2001) [hep-ex/0104049].
- [7] G. Garvey, E. Kolbe, K. Langanke and S. Krewald, Phys. Rev. C **48**, 1919 (1993).
- [8] S. D. Bass, Mod. Phys. Lett. A **24**, 1087 (2009) [arXiv:0905.4619 [hep-ph]].
- [9] A. A. Aguilar-Arevalo *et al.* [MiniBooNE Collaboration], Phys. Rev. D **82**, 092005 (2010) [arXiv:1007.4730 [hep-ex]].
- [10] R. Dharmapalan [MiniBooNE Collaboration], AIP Conf. Proc. **1405**, 89 (2011) [arXiv:1110.6574 [hep-ex]].
- [11] L. Bugel *et al.* [FINeSSE Collaboration], hep-ex/0402007.
- [12] A. A. Aguilar-Arevalo *et al.* [MiniBooNE Collaboration], Phys. Rev. D **81**, 092005 (2010) [arXiv:1002.2680 [hep-ex]].
- [13] C. Athanassopoulos *et al.* [LSND Collaboration], Phys. Rev. C **56**, 2806 (1997) [nucl-ex/9705002].
- [14] C. Athanassopoulos *et al.* [LSND Collaboration], Phys. Rev. C **55**, 2078 (1997) [nucl-ex/9705001].
- [15] B. Bodmann *et al.* [KARMEN Collaboration], Phys. Lett. B **280**, 198 (1992).
- [16] E. Kolbe, K. Langanke and P. Vogel, Nucl. Phys. A **652**, 91 (1999) [nucl-th/9903022].
- [17] A. A. Aguilar-Arevalo *et al.* [MiniBooNE Collaboration], Phys. Rev. D **83**, 052007 (2011) [arXiv:1011.3572 [hep-ex]].
- [18] A. A. Aguilar-Arevalo *et al.* [MiniBooNE Collaboration], Phys. Rev. D **83**, 052009 (2011) [arXiv:1010.3264 [hep-ex]].
- [19] A. A. Aguilar-Arevalo *et al.* [MiniBooNE Collaboration], Phys. Rev. D **81**, 013005 (2010) [arXiv:0911.2063 [hep-ex]].
- [20] J. A. Caballero, J. E. Amaro, M. B. Barbaro, T. W. Donnelly, C. Maieron and J. M. Udias, Phys. Rev. Lett. **95**, 252502 (2005) [nucl-th/0504040].

- [21] M. Martini, M. Ericson, G. Chanfray and J. Marteau, Phys. Rev. C **80**, 065501 (2009) [arXiv:0910.2622 [nucl-th]].
- [22] M. Martini, M. Ericson, G. Chanfray and J. Marteau, Phys. Rev. C **81**, 045502 (2010) [arXiv:1002.4538 [hep-ph]].
- [23] M. Martini, M. Ericson and G. Chanfray, Phys. Rev. D **85**, 093012 (2012) [arXiv:1202.4745 [hep-ph]].
- [24] C. Athanassopoulos *et al.* [LSND Collaboration], Nucl. Instrum. Meth. A **388**, 149 (1997) [nucl-ex/9605002].
- [25] A. A. Aguilar-Arevalo *et al.* [MiniBooNE Collaboration], Nucl. Instrum. Meth. A **599**, 28 (2009) [arXiv:0806.4201 [hep-ex]].
- [26] J. L. Raaf, E. A. Hawker, R. A. Johnson, A. O. Bazarko, G. T. Garvey, G. B. Mills, A. Pladalmu and R. Tayloe, IEEE Trans. Nucl. Sci. **49**, 957 (2002).
- [27] B. C. Brown *et al.* [MiniBooNE Collaboration], IEEE Nucl. Sci. Symp. Conf. Rec. **1**, 652 (2006).
- [28] MiniBooNE internal technical note, 116 (2004).
- [29] R. B. Patterson, E. M. Laird, Y. Liu, P. D. Meyers, I. Stancu and H. A. Tanaka, Nucl. Instrum. Meth. A **608**, 206 (2009) [arXiv:0902.2222 [hep-ex]].
- [30] MiniBooNE internal technical note, 74 (2003).
- [31] R. A. Reeder, B. D. Dieterle, C. Gregory, F. Schaefer, K. Schum, W. H. Strossman, D. Smith and L. Christofek *et al.*, Nucl. Instrum. Meth. A **334**, 353 (1993).
- [32] J. B. Birks, "The Theory and practice of scintillation counting," International series of Monographs on Electronics and Instrumentation, v. 27 Macmillan, New York.
- [33] G. Garino, M. Saber, R. E. Segel, D. F. Geesaman, R. A. Gilman, M. C. Green, R. J. Holt and J. P. Schiffer *et al.*, Phys. Rev. C **45**, 780 (1992).
- [34] B. D. Serot and X. Zhang, arXiv:1110.2760 [nucl-th].
- [35] B. D. Serot and X. Zhang, Phys. Rev. C **86**, 015501 (2012) [arXiv:1206.3812 [nucl-th]].
- [36] X. Zhang and B. D. Serot, arXiv:1208.1553 [nucl-th].
- [37] X. Zhang and B. D. Serot, arXiv:1206.6324 [nucl-th], accepted to Physical Review C.
- [38] J. A. Harvey, C. T. Hill and R. J. Hill, Phys. Rev. Lett. **99**, 261601 (2007) [arXiv:0708.1281 [hep-ph]].
- [39] R. J. Hill, Phys. Rev. D **81**, 013008 (2010) [arXiv:0905.0291 [hep-ph]].
- [40] X. Zhang and B. D. Serot, in Press.
- [41] R. J. Hill, Phys. Rev. D **84**, 017501 (2011) [arXiv:1002.4215 [hep-ph]].
- [42] A. A. Aguilar-Arevalo *et al.* [MiniBooNE Collaboration], Phys. Lett. B **664**, 41 (2008) [arXiv:0803.3423 [hep-ex]].